Chemical and Electrical Passivation of Silicon (111) Surfaces through Functionalization with Sterically Hindered Alkyl Groups

E. Joseph Nemanick, Patrick T. Hurley, Bruce S. Brunschwig, and Nathan S. Lewis*

210 Noyes Laboratory, 127-72, Division of Chemistry and Chemical Engineering, California Institute of Technology, Pasadena, California 91125

Received: December 5, 2005; In Final Form: May 10, 2006

Crystalline Si(111) surfaces have been alkylated in a two-step chlorination/alkylation process using sterically bulky alkyl groups such as $(CH_3)_2CH-$ (*iso*-propyl), $(CH_3)_3C-$ (*tert*-butyl), and C_6H_5- (phenyl) moieties. X-ray photoelectron spectroscopic (XPS) data in the C 1s region of such surfaces exhibited a low energy emission at 283.9 binding eV, consistent with carbon bonded to Si. The C 1s XPS data indicated that the alkyls were present at lower coverages than methyl groups on CH_3-terminated Si(111) surfaces. Despite the lower alkyl group coverage, no Cl was detected after alkylation. Functionalization with the bulky alkyl groups effectively inhibited the oxidation of Si(111) surfaces in air and produced low (<100 cm s^{-1}) surface recombination velocities. Transmission infrared spectroscopy indicated that the surfaces were partially H-terminated after the functionalization reaction. Application of a reducing potential, -2.5 V vs Ag^+/Ag, to Cl-terminated Si(111) electrodes in tetrahydrofuran resulted in the complete elimination of Cl, as measured by XPS. The data are consistent with a mechanism in which the reaction of alkyl Grignard reagents with the Cl-terminated Si(111) surfaces involves electron transfer from the Grignard reagent to the Si, loss of chloride to solution, and subsequent reaction between the resultant silicon radical and alkyl radical to form a silicon−carbon bond. Sites sterically hindered by neighboring alkyl groups abstract a H atom to produce Si−H bonds on the surface.

I. Introduction

A variety of procedures have recently been developed to alkylate Si surfaces in attempts to passivate crystalline Si surfaces toward oxidation and to impart other desirable properties to this widely used semiconductor. The H-terminated Si(111) surface has been immersed in terminal alkenes or alkynes to form Si−C bonds through free-radical reactions initiated thermally[1−4] or photochemically,[5−7] and through Lewis acid-catalyzed hydrosilylation[8,9] or transition-metal-catalyzed[10] reactions. Other alkylation strategies involve formation of surficial Si radicals with scanning tunneling microscopy,[11] atomic force microscopy,[12] or mechanical scribing[13] of the surface, and subsequent reaction of these radicals with alkenes or alkynes. Several electrochemical methods have also been shown to form surface-bonded alkyl groups.[14−16]

Surfaces alkylated using a two-step chlorination/alkylation process with straight-chain alkyl groups (C_nH_{2n+1}, $n = 1-8$) have shown excellent surface passivation both from a chemical viewpoint and from an electrical viewpoint.[5,17−22] In this process, the H-terminated Si(111) surface is first chlorinated to make a metastable surface, and this surface is then reacted with organolithium or Grignard reagents to form the desired Si−C-terminated surfaces. The distance between Si atop atoms on an unreconstructed 1×1 H-terminated Si(111) surface is 3.8 Å,[23] while the van der Waals radius of a methyl group is approximately 2.0 Å.[24] Hence, a methyl group can, in principle, react with every Si atop site on the unreconstructed Si(111) surface. Indeed, the CH_3−Si(111) surface prepared through the two-step chlorination/alkylation method has been observed using scanning tunneling microscopy methods to show a nearly complete coverage of methyl groups, in a 1×1 pattern, over wide regions of the surface.[25] In contrast, the van der Waals radius of the $Si-CH_2CH_2-$ moiety, or of any functionality with methylene groups (i.e., C_nH_{2n+1}, $n \geq 2$), is larger than 2.5 Å. Hence, on the Si(111) surface, complete functionalization of Si atop sites with methylene-containing alkyl groups would face severe steric difficulties.

Despite this steric constraint, Si(111) surfaces alkylated with straight-chain alkyl groups have shown enhanced stability toward oxidation and have also shown low surface recombination velocities.[17,18,22] Interestingly, no Cl signal is present by X-ray photoemission spectroscopy (XPS) after the alkylation process.[22] Bulkier, nonstraight-chain functional groups, such as *tert*-butyl or phenyl, are subject to even more severe packing limitations on the Si(111) surface. In this work, we describe the preparation of Si(111) surfaces alkylated with $C_nH_{2n+1}-$ ($n = 1$, 2, and 8), $(CH_3)_2CH-$ (*iso*-propyl), $(CH_3)_3C-$ (*tert*-butyl), and C_6H_5- (phenyl) groups. The resulting surfaces have been characterized by X-ray photoelectron spectroscopy (XPS), surface recombination velocity (SRV) measurements, attenuated total reflectance surface infrared (ATR−IR) absorption spectrometry, and cyclic voltammetry. The alkylated Si surfaces were monitored for the rate of electron−hole recombination by SRV measurements and for their rate of oxidation by XPS. Cyclic voltammetry experiments and ATR−IR have been used to provide insight into the mechanism of the alkylation reaction in such systems.

II. Experimental Section

A. Alkylation of Silicon. The silicon samples used for SRV and XPS measurements were float-zone grown, (111)-oriented

* Author to whom correspondence should be addressed. Ph: 626-395-6335. Fax: 626-395-8867. E-mail: nslewis@its.caltech.edu.

10.1021/jp057070i CCC: $33.50
Published on Web 07/13/2006

wafers that were polished on both sides (Virginia Semiconductor, Fredericksburg, VA). To minimize the bulk contribution to charge-carrier recombination, 250-μm-thick, high-resistivity (>4000 Ω cm), n-type, phosphorus-doped silicon was used. Prior to alkylation, samples were cut into sections ~1 cm^2 in area. The pieces were cleaned by sonication for 5 s in a series of organic solvents (VWR Scientific Products, West Chester, PA): methanol, acetone, dichloromethane, 1,1,1-trichloroethane, dichloromethane, acetone, and methanol, and then 18-MΩ·cm resistivity H_2O. To produce a H-terminated surface, the samples were then etched for 30 s in buffered HF(aq). Samples were then etched, with occasional agitation to remove bubbles forming on the edges, for 10 min in 40% NH_4F(aq) (Transene, Danvers, MA). After etching, the samples were dried under a stream of N_2(g) and passed into a glovebox for functionalization.

To chlorinate the surfaces, samples were immersed in 2 mL of anhydrous chlorobenzene (99.8% under argon, Aldrich) saturated with PCl_5 (99.995%, Strem, Newburyport, MA) for 1 h at 95−100 °C. Benzoyl peroxide (97%, Aldrich) was added (<1 mg) to initiate the chlorination of the surface. Care was taken to ensure that the polished surfaces of the silicon samples were not touched, to prevent scratching that might influence the surface reactivity.

After chlorination, the samples were washed in anhydrous tetrahydrofuran (THF) (99.8%, inhibitor-free, Aldrich) and were placed in Teflon screw-cap sealed glass reaction flasks that contained 10 mL of anhydrous THF and 10 mL of a 1 M Grignard reagent in THF. The Grignard reagents were either CH_3MgCl, CH_3CH_2MgCl, $CH_3(CH_2)_7MgCl$, $(CH_3)_2CHMgCl$, $(CH_3)_3CMgCl$, or C_6H_5MgCl. The reaction solution was heated to 110−120 °C for 21 h in a sealed reaction vessel. After reaction, samples were rinsed in THF and then by anhydrous methanol (99.8% Aldrich), removed from the glovebox, and sonicated in a 5-mL solution of methanol and glacial acetic acid (10:1) (Aldrich) for 5 min to remove any adsorbed magnesium salts. Samples were then rinsed with 18-MΩ·cm resistivity H_2O and either passed directly into the ultrahigh vacuum (UHV) load lock for XPS analysis or placed in scintillation vials for SRV measurements.

B. Electrochemistry. Electrodes were fashioned from 550-μm-thick, double-side-polished, n-type (As-doped), prime grade Si(111) with a resistivity of <0.004 Ω·cm (Addison Engineering Corp, San Jose, CA). Samples were cut into 1−3-cm^2 squares, and an ohmic contact was formed by the application of a Ga−In (Aldrich) eutectic on an etched portion of the silicon. Silver print was used to attach a tinned Cu lead wire to the eutectic-coated back surface of the Si. The lead wire was then encased in glass tubing and sealed in epoxy.

Electrochemistry was performed in a three-electrode configuration with a Pt coil counter electrode and a Ag^+/Ag reference electrode. The electrolyte, unless otherwise noted, was 100 mM tetra(*n*-butyl)ammonium hexafluorophosphate ($TBAPF_6$, Fluka, electrochemical grade) in THF (J. T. Baker, Phillipsburg, NJ, Ultra Low Water, BakerDry). The Ag^+/Ag reference electrode consisted of a saturated solution of silver nitrate (99.999%, Aldrich) in the THF electrolyte with a Ag wire. The reference compartment was separated from the electrochemical solution by a Vycor frit. The working electrode was either Pt (0.071-cm^2 surface area) or silicon. All electrochemistry was performed under anaerobic conditions in a glovebox with <10 ppm of O_2. Unless otherwise noted, cyclic voltammograms were taken at 150 mV s^{-1} on a Solartron 1287 potentiostat (Solartron Analytical, Farnborough, UK) with data collected using Corrware, v 2.5b (Scribner Associates). Cyclic voltammograms and potentiostatic experiments on silicon working electrodes were carried out in the dark. After electrochemical measurements, the electrodes were rinsed in THF, dried under a stream of flowing N_2(g), scribed below the epoxy sealant, and broken into squares for XPS measurements.

C. X-ray Photoelectron Spectroscopy. XPS data were collected on a UHV system that has been described previously.[18] The collection chamber was maintained at ≈5 × 10^{-10} Torr when not in use, whereas due to sample outgassing the pressure rose to ≈2 × 10^{-8} Torr during data collection. Due to the relatively low resistivity of the samples, charge compensation was not needed. All measurements were taken on the center of the sample to ensure reproducibility and to minimize the effects of scratches or contamination at the edges. The incident beam consisted of 1486.6-eV X-rays from an Al Kα source, and ejected electrons were collected at 55° off of the surface normal. All energies are reported as binding energies in eV. The XPS system was periodically calibrated using the 4f peaks of a Au standard at 83 and 87 binding eV.

Data were collected using ESCA 2000 E Capture software, v. 102.04 (Service Physics). Samples were first scanned from 0 to 1000 binding eV to monitor signals for Cl as well as C and O. The Si 2p, Cl 2p, and C 1s regions of 98−105, 198−204, and 282−287 binding eV, respectively, were investigated in detail. The Si 2p region was used to monitor the growth of Si oxides. Scan times of up to 4 h were employed for data collection. The spectrometer resolution was ≈0.5 eV.

Oxide coverages were determined by integration of the area under the broad oxygen-shifted Si 2p peak centered around 103 binding eV, which was comprised of SiO_2 and Si suboxides. This peak area was ratioed to the area of the bulk Si $2p_{3/2}$ and Si $2p_{1/2}$ peaks. Using ESCA 2000 A Analysis, v. 102.04 integration software, the peak shapes were fitted to Voigt functions fixed at 95% Gaussian and 5% Lorentzian line shapes. The position of the Si $2p_{1/2}$ peak was fixed at 0.6 binding eV higher than the $2p_{3/2}$ peak, and the full width at half maximum (fwhm) was constrained to be identical to that of the Si $2p_{3/2}$ peak, with the total integrated area ratio of the $2p_{1/2}/2p_{3/2}$ peaks fixed at 0.51.[17]

The fractional monolayer coverage of oxide species on the surface was determined using the substrate−overlayer model:[26]

$$\frac{d_o}{d_1} = \lambda_O \sin\theta \left\{ \ln\left[1 + \left(\frac{I_{Si}^{\,0}}{I_O^{\,0}}\right)\left(\frac{I_O}{I_{Si}}\right)\right]\right\} \qquad (1)$$

where d_o is the overlayer thickness, d_1 is the thickness of one monolayer of oxide (3.5Å), and λ_O is the attenuation factor of the oxide layer (26 Å). θ is the takeoff angle for the measurement (90° − 55°, i.e., 35°), $I_{Si}^{\,0}/I_O^{\,0}$ is a normalizing factor for the particular instrument used (1.3 for this instrument[17]), and I_O/I_{Si} is the ratio of the peak area of the oxide-shifted silicon to the area of the unshifted silicon peak.

Data from the carbon 1s emission region were fitted to three peaks, representing silicon-bonded carbon at 283.9 eV, carbon-bonded carbon at 285.0 eV, and oxygen-bonded carbon at 286.8 eV. Peaks were fitted to Voigt functions having 70% Gaussian and 30% Lorentzian character. The peak centers were allowed to float, though the center-to-center distances were fixed at 1.1 eV between the silicon-bonded carbon and the carbon-bonded carbon emissions, and at 1.8 eV between the oxygen-bonded carbon and the carbon-bonded carbon emissions. The integrated area under each carbon peak was ratioed to the integrated area under the silicon 2p peaks for that sample, normalized for scan time. The ratio of the silicon-bonded carbon to the normalized

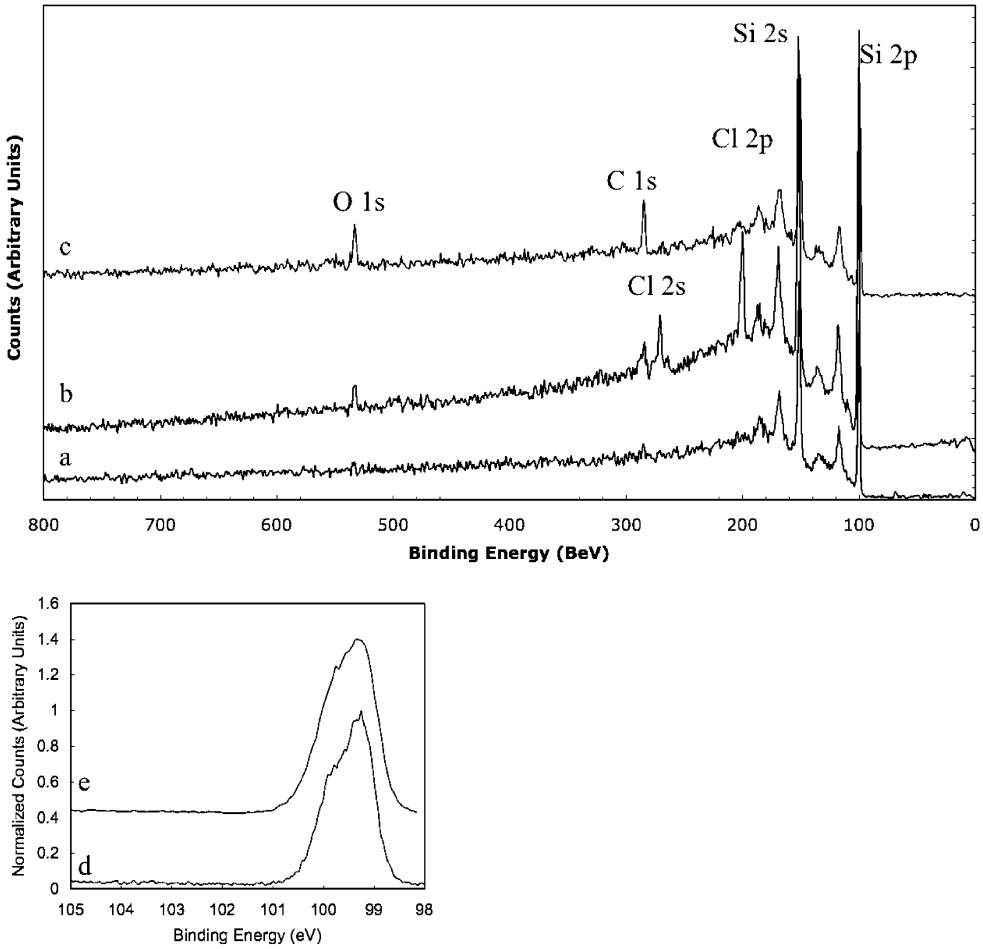

Figure 1. XPS spectra of (a) H-terminated Si(111), (b) Cl-terminated Si(111), (c) CH_3-terminated Si(111), (d) the silicon 2p region for H−Si, and (e) the Si 2p region of CH_3−Si surfaces.

area for the Si 2p peak (C_{Si}/Si) was then compared between alkylated surfaces. The methyl-terminated Si(111) surface was used as a reference surface for the other alkylated Si surfaces, so surface coverages for each alkyl group are reported as $(C_{Si}/Si)_{alkyl}/(C_{Si}/Si)_{methyl}$.

D. Infrared Spectroscopy. For IR spectroscopy, n-type, phosphorus-doped, float-zone, single-crystal, 505 ±25-μm-thick Si(111) wafers (Silicon Valley Microelectronics Inc., Santa Clara, CA) with a resistivity of >30 Ω·cm were cut into 2.1 × 3-cm segments. Samples were cleaned with an RCA etch, before a final etch in degassed 40% NH_4F(aq) for 20 min. Surfaces were chlorinated and alkylated as described above, with samples sealed under N_2 for transport to the FT-IR. Samples were unsealed and placed in a GATR mount (Herrick Scientific Products Inc., Pleasantville, NY) for grazing angle (65°) ATR spectroscopy. The GATR mount was placed in a Vertex 70 FT-IR spectrometer (Bruker Optics Inc., Billerica, MA) for measurements. A total of 512 scans for each sample were taken in air, with background scans of air subtracted from the spectra.

E. Surface Recombination Velocity Measurements. Surface recombination velocity measurements were collected using a contactless rf conductivity apparatus.[19] Samples were excited with 10-ns pulses at 1064 nm from a Nd:YAG laser operating at 10 Hz. The photogenerated electron−hole pairs diffused to either surface of the sample to recombine through surface-localized electronic states within the Si band gap. The bulk charge-carrier lifetimes as reported by the manufacturer (~6 ms) were much longer than the observed lifetimes, indicating that charge-carrier recombination effectively only occurred at the silicon surfaces. Charge-carrier concentrations were monitored by measuring the reflected signal from a 450-MHz rf coil. The absorbed rf signal was recorded by averaging 128 traces, and the data were fitted to a single-exponential decay:

$$A = y_o + ae^{-t/\tau} \tag{2}$$

where τ is the observed charge-carrier lifetime. The surface recombination velocity, S, is obtained from τ through

$$\frac{1}{\tau} = \frac{1}{\tau_b} + \frac{2S}{d} \tag{3}$$

where τ_b is the bulk lifetime, and d is the sample thickness. For all measurements, $\tau_b \gg \tau$, so $S \approx d/2\tau$.

All τ values are reported after the first 24 h following alkylation. Initial measurements of τ for an individual sample showed a slight increase in charge-carrier lifetime over the first day, but stabilized thereafter. To monitor the stability of the alkylated surface toward oxidation, samples were stored in scintillation vials under laboratory air and normal laboratory illumination conditions for up to 71 days, and τ values were monitored periodically during this time interval.

III. Results

A. XPS Data. Figure 1 shows representative XPS data for the two-step chlorination/alkylation of Si(111) surfaces. H-terminated surfaces exhibited peaks for elemental silicon 2s (150-eV) and 2p (100-eV) emissions as well as the silicon

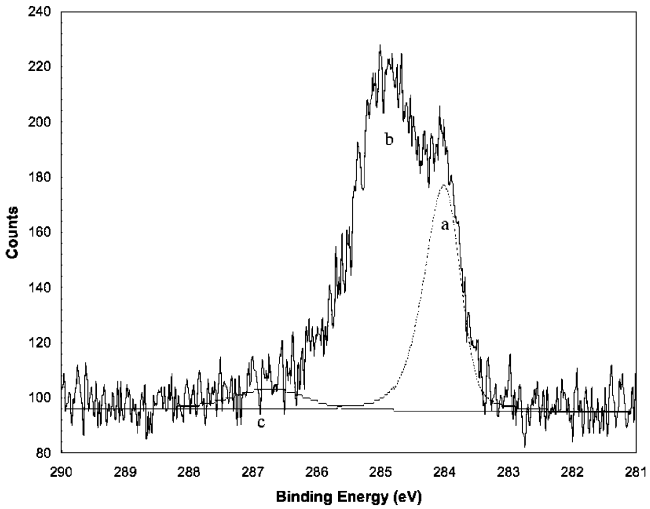

Figure 2. XPS data of the carbon 1s region of an C_2H_5-terminated Si(111) surface with peaks fits (dashed lines) for (a) carbon bonded to silicon, (b) carbon bonded to carbon (and hydrogen), and (c) carbon bonded to oxygen.

phonon emission bands at 17 and 36 eV above the 2s and 2p peaks, respectively. Trace amounts of C and O were observed at 284 and 532 eV, respectively. The Cl 2p and 2s peaks, at 201 and 271 eV, respectively, appeared after the chlorination step. After alkylation, no Cl peaks were observed, and the C 1s peak increased in amplitude. No oxidized silicon was detected in detailed scans of the Si 2p region, indicating that the submonolayer amounts of oxygen present were bonded to adventitious C sources resulting from the alkylation process and not from oxidation of the Si surface.

Figure 2 shows a high-resolution XPS scan of the C 1s region of an ethylated surface. Two main peaks were observed at 283.9 and 285.0 eV, with a third, small signal at 286.8 eV. The peaks at 285.0 and 286.8 eV were common to alkylated and H-terminated silicon surfaces, whereas the low binding energy peak at 283.9 eV was unique to alkylated Si surfaces. Hence, the peak at 283.9 eV can be assigned to emission from core-level electrons of carbon atoms covalently bonded to the relatively electropositive silicon.[5,27] The higher energy peak at 285.0 eV can be ascribed to carbon in a nonpolar bond with either hydrogen or another carbon atom. This carbon peak was the sum of C 1s electrons from adventitious carbon sources as well as alkylating carbons that do not participate in the Si−C bond. The appearance of a third C 1s peak shifted to higher binding energy at 286.8 eV is ascribed to adventitious carbon bonded to oxygen. The higher binding energy C 1s peaks also contain contributions from vibrational excitations of the C 1s peaks with lower binding energies.[5,27] The ratio of the O 1s peak in the survey scan to the peak area of the C 1s emission at 286.6 eV was generally ≈2:8, which is in accord with the expected ratio given the different sensitivity factors for C 1s and O 1s with a 1:1 stoichiometry between the oxygen of the O 1s signal and the full area of the 286.6-eV oxidized C 1s peak.

The assignment of the emission at 283.9 eV to the C 1s peak of silicon-bonded carbon (C_{Si}) enabled a quantitative measurement of the relative coverage of surficial Si−C bonds on the various alkylated surfaces. Table 1 presents the peak area ratio of the silicon-shifted carbon signal to the Si 2p signal (C_{Si}/Si) for each alkyl group, relative to the C_{Si}/Si peak ratio for the methylated surface. Methylation has been shown by various methods to provide a nearly complete monolayer on the Si-(111) surface.[25,27−29] Ethylated surfaces showed a C_{Si}/Si peak ratio of 90 ± 20% relative to that of CH_3-terminated Si surfaces,

TABLE 1: C_{Si}/Si XPS Integrated Area Ratios for Alkylated Surfaces Showing the Relative Amount of Carbon Bonded to Silicon for Each Alkyl Surface[a,b]

	ratio C_{Si}/Si	% of methyl coverage
methyl	0.16 ± 0.02	
ethyl	0.14 ± 0.02	(9 ± 2) × 10[1]
iso-propyl	0.06 ± 0.02	(4 ± 2) × 10[1]
tert-butyl	0.061 ± 0.008	(4 ± 2) × 10[1]
phenyl	0.08 ± 0.02	(5 ± 2) × 10[1]
octyl	0.092 ± 0.008	(6 ± 1) × 10[1]

[a] Standard deviations are over four samples. [b] Surface coverages are reported relative to the methylated surface.

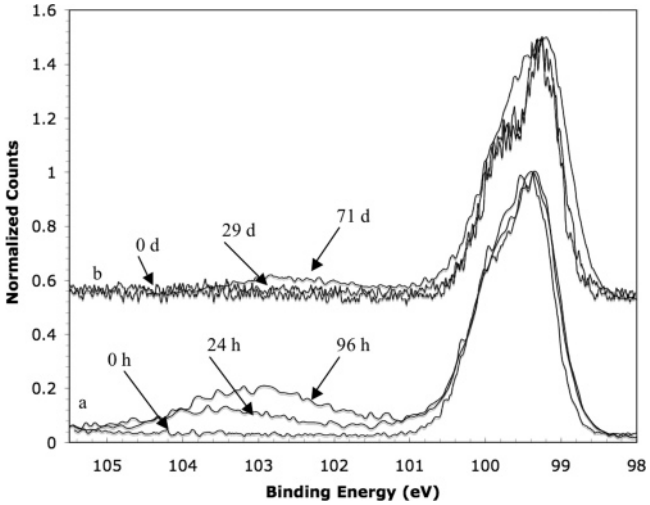

Figure 3. XPS data of the oxidation of the Si(111) 2p region for (a) H-terminated Si(111) at 0, 24, and 96 h in air, and (b) CH_3-terminated Si(111) at 0, 29, and 71 days in air.

indicating that ethyl groups can be packed at a very high density by this two-step alkylation method. Octyl and phenyl produced 60 ± 10% and 50 ± 20%, respectively, of the methyl coverage, while alkylation with *tert*-butyl and *iso*-propyl groups produced 40 ± 20% and 40 ± 20% of the C_{Si}/Si ratio of methyl-terminated Si.

Figure 3 shows the evolution of the XPS spectra of alkylated Si surfaces as a function of time exposed to ambient air. Oxidation of the Si surface was monitored by the growth of the broad Si^{x+} peak between 101 and 105 BeV. Relative to H-terminated Si, CH_3-terminated Si surfaces exposed to air in the dark over a period of more than two months showed greatly reduced surface oxidation. The surface oxidation for other alkylated Si surfaces is shown in Figure 4. All alkylated surfaces showed similar oxidation rates, with no discernible differences correlating to alkyl coverage or size of the alkyl group.

B. Surface Recombination Velocity Measurements. Table 2 shows the average charge-carrier lifetimes for the alkylated and H-terminated surfaces exposed to air over a 24-day interval. Lifetimes for air-exposed (oxidized) H-terminated Si(111) surfaces were less than 10 μs, the lower limit for the measurement technique, indicating that all charge-carriers recombined upon reaching the surface, with the observed lifetime dominated by diffusion of charge-carriers to the electrically active surface regions. For all the alkylated surfaces, the charge-carrier lifetimes were extremely long. Charge-carrier lifetimes for these samples were still significantly less than the manufacturer's reported bulk lifetimes (∼6 ms), implying that recombination even for the alkylated surfaces still occurred almost exclusively at the surface.

All of the alkylated surfaces exhibited substantially lower surface recombination velocities (<100 cm s^{-1}) relative to air-

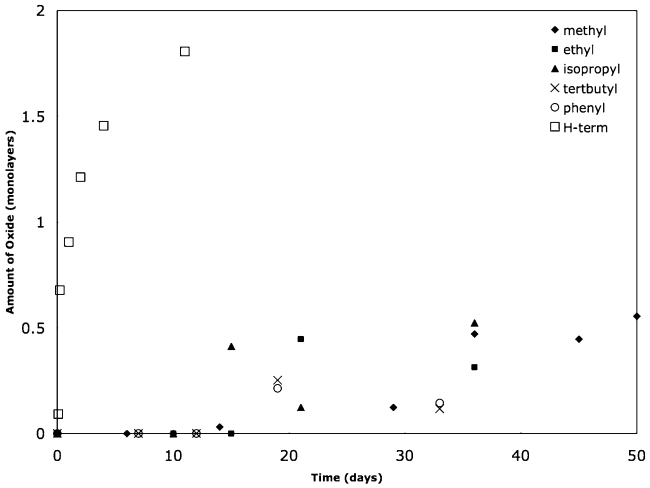

Figure 4. Surface oxide growth for H-terminated and alkylated Si(111) surfaces vs time in air, showing the rapid oxidation of the H−Si(111) surface as compared to alkylated Si(111) surfaces.

TABLE 2: Charge-Carrier Lifetimes for Alkylated Surfaces after 24 Days in Air[a]

	charge-carrier lifetime τ (μs)	surface recombination velocity S (cm s^{-1})
methyl	$(2.3 \pm 0.4) \times 10^2$	44 ± 9
ethyl	$(1.8 \pm 0.5) \times 10^2$	$(6 \pm 2) \times 10^1$
iso-propyl	$(2.0 \pm 0.5) \times 10^2$	$(6 \pm 2) \times 10^1$
tert-butyl	$(1.6 \pm 0.6) \times 10^2$	$(8 \pm 4) \times 10^1$
phenyl	$(2.0 \pm 0.9) \times 10^2$	$(6 \pm 2) \times 10^1$
H-terminated	<10	$>1 \times 10^3$

[a] H-terminated Si(111) samples had charge-carrier lifetimes shorter than could be measured by the rf conductivity apparatus.

oxidized H-terminated Si(111) surfaces (>1000 cm s^{-1}; Table 2). No clear trend was observed with respect to alkyl chain length or bulk, and all values are within experimental error, separated only from H−Si(111) at <10 μs. Over the course of measurement, the charge-carrier lifetimes initially increased and then declined over time. The decline in τ may result from introduction of surface-based recombination sites by either slow oxidation of the surface or due to sample handling. Figure 5 shows the progression of the charge-carrier lifetimes for methylated and *tert*-butylated surfaces, superimposed on the surface oxidation of the samples as measured by XPS. The measured lifetimes of the alkylated samples remained extremely high ($\approx$200 μs) even at significant levels of oxidation, indicating that samples which have half a monolayer of oxidized silicon at the surface do not exhibit significant increases in surface recombination velocities.

C. Infrared Spectroscopy. Figure 6 shows ATR infrared absorbance spectra of the (111)-oriented Si surfaces alkylated with ethyl and *tert*-butyl groups. The well-known Si−H stretch at $\approx$2100 cm^{-1} disappeared completely after chlorination and was not apparent after alkylation with methyl groups.[30] However, the Si−H stretch was observed after functionalization with the larger groups *tert*-butyl and ethyl.

D. Electrochemical Studies. The reactivity of Cl-terminated Si(111) surfaces was investigated to elucidate the mechanism of the reaction between the Grignard alkylating reagents and the surficial Si−Cl bonds. The surficial Si−Cl bonds form a monolayer coverage for surfaces that have been chlorinated with PCl_5.[28]

Figure 7 compares the cyclic voltammetry of a chlorinated Si(111) surface with that of a Pt electrode in THF. The chlorinated silicon electrode showed an irreversible reductive peak at −2.5 V vs Ag^+/Ag. This peak decreased in size with successive sweeps, indicating that the reducible species was in finite supply at the electrode. Taking the surface density of a full monolayer of chlorinated atoms as the density of Si atop sites on an unreconstructed Si(111) (1 × 1) surface (7.8×10^{14} atoms per cm^2), integration of the areas under the successive reductive peaks yielded 0.8 ± 0.3 electrons per surface site. This indicates that the reduction current results from the one-electron reduction of the Si−Cl species.

Figure 8 displays the XPS data of a Cl−Si(111) electrode after the potentiostatic application of either −1.0 or −2.5 V vs Ag^+/Ag for 10 min in THF. The electrode exposed to −1.0 V showed significant Cl 2s and 2p signals, while the surface exposed to −2.5 V showed no residual Cl wide-scan XPS signals. Detailed scans of the Cl 2p region (Figure 8 inset) showed the complete removal of the Cl 2p spin−orbit doublet.

The Grignard reagents used for alkylation are strongly reducing compounds and show broad, irreversible oxidative waves in their cyclic voltammograms between −2.5 and −1.5 V vs Ag^+/Ag (Figure 9). The overlap of these oxidative waves with the reductive wave observed for the Cl-terminated Si(111) surface indicates that the Grignard reagents have a sufficiently reducing electrochemical potential to reduce the chlorine bonds on the Cl−Si(111) surface.

IV. Discussion

A. Coverage of Alkyl Groups on Functionalized Si(111) Surfaces. The C 1s XPS signals on alkylated Si(111) surfaces reflect both alkyl carbons bonded to Si and adventitious C physisorbed on the surface. Resolution of the various carbon signals is possible because the C binding energy shifts with the nature of the atom(s) bound to the carbon center. These shifts result from differences in the effective charge on the C. Because Si−C bonds are appreciably more polar than C−C or C−H bonds (the Pauling electronegativities for carbon, hydrogen, and silicon are 2.55, 2.2, and 1.90, respectively[31]), a C bound to Si is relatively more negative than a C bound to C or H. Thus a lowered binding energy is observed for C bound to Si than for to C bound to C or H. The low binding energy peak observed for alkylated Si surfaces in the C 1s region was therefore identified with a C bonded to Si, and this signal was used to estimate the packing density of the alkyl groups on the functionalized silicon surface.

As expected, the bulky alkyl groups were present at a lower surface coverage than methyl groups on CH_3-terminated Si(111) surfaces. Functionalization with C_2H_5- groups produced a coverage of silicon-bonded carbon which was $90 \pm 20\%$ of that observed for CH_3-terminated Si(111) surfaces. These data contrast with simple models for functionalized Si(111) surfaces, which suggest that steric restrictions imposed by the bent Si−C−C bonds will limit the surface packing for ethyl to approximately 50% of surface sites.[1,32] Molecular modeling studies of alkylations performed by addition of olefins to H−Si(111) surfaces, constrained to coverages that produce negligible bond strain in the resulting overlayer, have suggested that an upper limit on the coverage for alkyls is $\approx$50% of a monolayer. The observed coverage for C_2H_5- of in excess of 80% of a monolayer can be accounted for by at least two factors. STM images of Si(111) surfaces produced by the two-step chlorination/alkylation method indicate that such surfaces have approximately 16% of the atoms on step edges or in etch pits,[25]

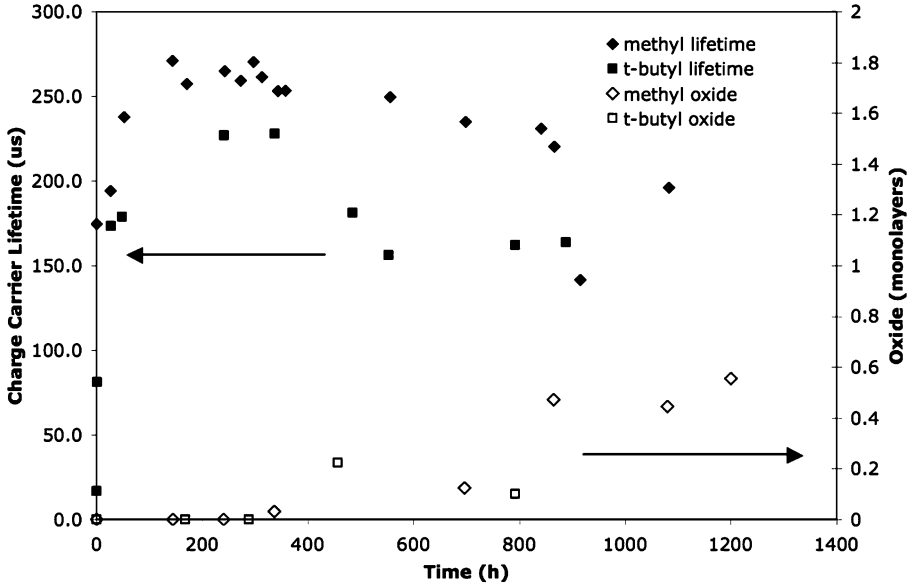

Figure 5. Charge-carrier lifetimes for CH_3- and $(CH_3)_3C$-terminated Si(111) surfaces vs surface oxide growth. Alkylated surfaces often exhibited an increase in charge-carrier lifetime over the first day and a gradual decline over time. Samples did not show a significant loss in their charge-carrier lifetime as the surface oxidized.

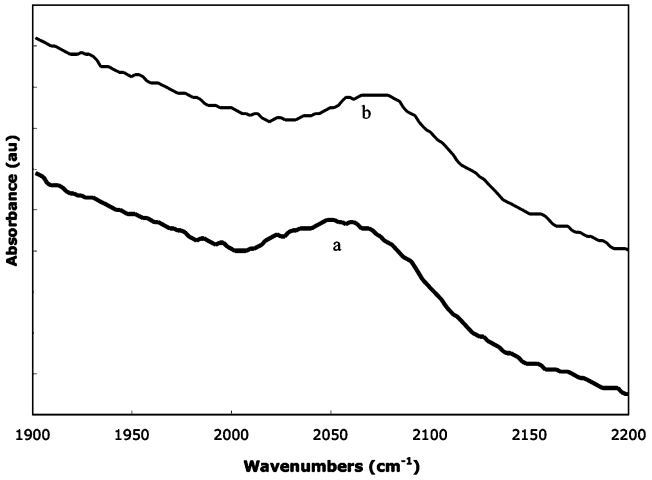

Figure 6. IR absorbance in arbitrary units showing the Si−H stretch for (a) C_2H_5-terminated Si(111) surfaces and for (b) *tert*-butyl-terminated Si(111) surfaces.

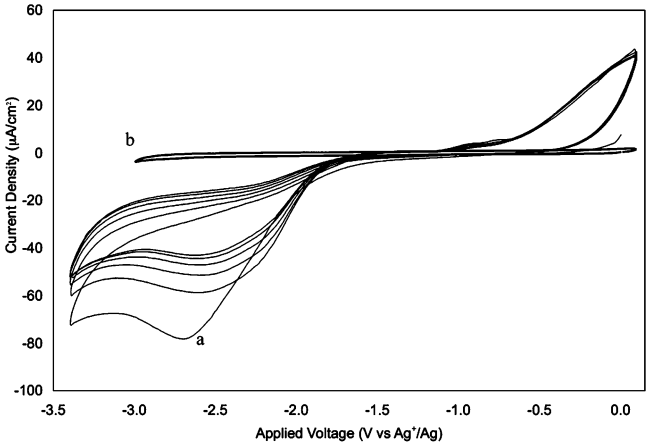

Figure 7. Cyclic voltammetry of (a) a Cl-terminated Si(111) electrode showing a prominent irreversible reductive peak at ∼−2.5 V and (b) a Pt working electrode in the same solution. The area under the reductive peaks for Si−Cl electrodes was 0.8 ± 0.3 e^- per surface site.

thereby providing a possibility for strain relief relative to a perfect surface consisting of only terrace atoms. Additionally, the reaction of the Grignard reagents with the Cl-terminated Si surface is highly exothermic, and significant bond strain can therefore be accommodated in the product state of the alkylated surface formed by this route. Evaluating the relative contributions of these two factors to the observed coverage will require the formation of nearly defect-free, highly terraced surfaces by a nearly thermoneutral reaction route.

Although octyl and ethyl groups should have similar footprints on the Si surface, as determined by the tetrahedral bonding at the terminal silicon-bound carbon, the surface coverage for octyl was significantly less, 60 ± 10% of that for CH_3−Si-(111). Steric interactions between the long tails of the bound octyl groups will increase with each successive octyl group. Because these steric interactions increase with tail length, fewer octyl groups than ethyl groups are expected to bind to the surface. The *iso*-propyl moiety was observed to bond to even fewer of the surface sites (40 ± 20% relative to CH_3−Si(111)) than octyl, even though both ethyl and *iso*-propyl have only a CH_3− tail. The addition of another CH_3− group bound to the silicon-bonded carbon atom, however, forces the *iso*-propyl group to bind to the surface with its two CH_3− groups projecting more laterally over the surface. This larger footprint relative to $-C_2H_5$ restricts binding to adjacent silicon atoms, resulting in a relatively low coverage of *iso*-propyl groups on Si atop sites. Thus, surface alkylation can be inhibited both by tail−tail interactions as the alkyl groups get longer, and by overlap of neighboring silicon atoms on branched alkyl groups.

B. Mechanism of Alkylation of Cl-Terminated Si(111) Surfaces by Grignard Reagents. For the two-step alkylation reaction, functionalization of the silicon surface with alkyl groups proceeds though the Cl-terminated Si(111) surface. The alkylation of the chlorinated surface results in the complete removal of Cl by XPS, regardless of the size of the alkyl group.

Cl-terminated Si(111) surfaces were observed to be robust in sealed reaction vessels toward hot (120 °C) THF and showed by XPS no significant loss of Cl after 21 h. The first step of the reaction between the Grignard reagents and the Cl-terminated Si(111) surface therefore cannot be abstraction of chlorine by solvent molecules or a pure S_N1-type reaction. Nor could

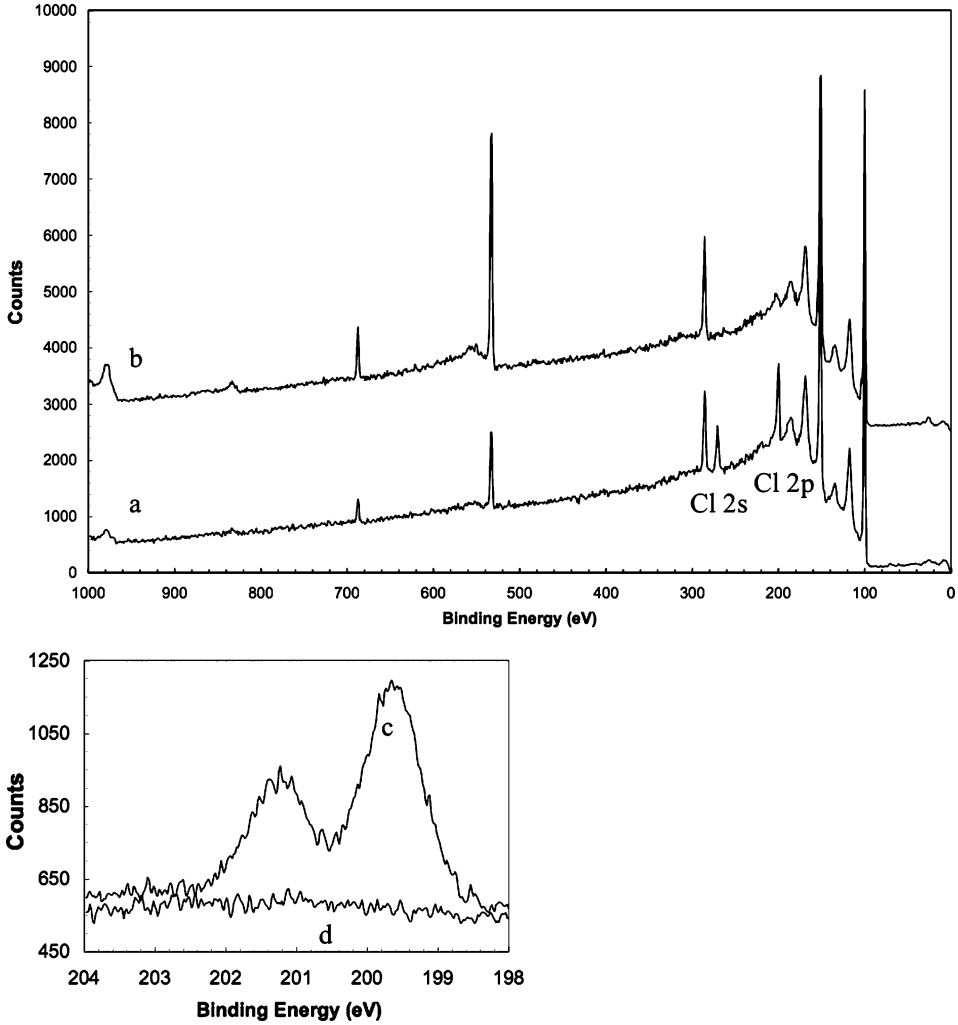

Figure 8. XPS data of (a) a Cl-terminated Si(111) electrode subjected to −1 V vs Ag^+/Ag for 10 min in THF with 100 mM $TBAPF_6$, (b) a Cl-terminated Si(111) electrode held at −2.5 V in the same solution, (c) the chlorine 2p region for the electrode in (a), and (d) the Cl 2p region for the electrode in (b). These spectra show the total removal of surficial chlorine only after sufficient reducing potential. The small peak visible in (b) at ∼201 binding eV is due to a phonon absorption band present in bulk silicon.

abstraction of Cl proceed through the direct attack by the alkyl Grignard reagent on a Cl atom, because a large alkyl group, such as octyl, would be unable to reach every surface chlorine atom after partial surface alkylation had occurred. Hence, steric constraints argue against the reaction of the Cl−Si(111) surface with the Grignard reagent occurring by an S_N2-type mechanism through a 5-coordinate intermediate on the front side of the Si. Additionally, the Grignard reagent has no access to the back of the Si−Cl site due to the presence of the bulk crystal.

A mechanism consistent with the data involves electron transfer to the silicon surface followed by chemical reaction of a reduced surficial Si−Cl. As shown in Figure 9, the Grignard alkylating reagents have sufficiently negative reduction potentials to reduce the Cl-terminated Si(111) surface. Electrochemical reduction at these potentials clearly results in removal of all of the surface Cl atoms (Figure 8). Due to the conductive nature of the doped silicon, electron transfer could occur at locations removed from the Si−Cl bond that is ultimately reduced, providing a mechanism to explain the observed reactivity of all of the Cl-terminated sites with the hindered alkyl Grignard reagents.

A mechanism consistent with the observations presented herein consists of the following four steps:

Step 1:

$$\mathrm{Si{-}Cl} + \mathrm{e^-} \rightarrow [\mathrm{Si{-}Cl}]^- \rightarrow \mathrm{Si\cdot} + \mathrm{Cl^-}$$

Step 2:

$$\mathrm{RMgCl} + \mathrm{h^+} \rightarrow [\mathrm{RMgCl}]^+ \rightarrow \mathrm{R\cdot} + [\mathrm{MgCl}]^+$$

Step 3:

$$\mathrm{Si\cdot} + \mathrm{R\cdot} \rightarrow \mathrm{Si{-}R}$$

Step 4:

$$\mathrm{Cl^-} + [\mathrm{MgCl}]^+ \rightarrow \mathrm{MgCl_2}$$

Steps (1) and (2) would be (nearly) simultaneous, with reduction of the Si−Cl bond by the Grignard reagent leading to the removal of Cl from the surface, as well as creating alkyl radicals for subsequent reaction. This type of single-electron-transfer reaction (SET) for Grignard reagents is well-known and produces alkyl radicals.[33−36] Step (3) yields the expected alkylated surface. For silicon sites that cannot be accessed by the larger alkyl radicals, the silicon radical would abstract a

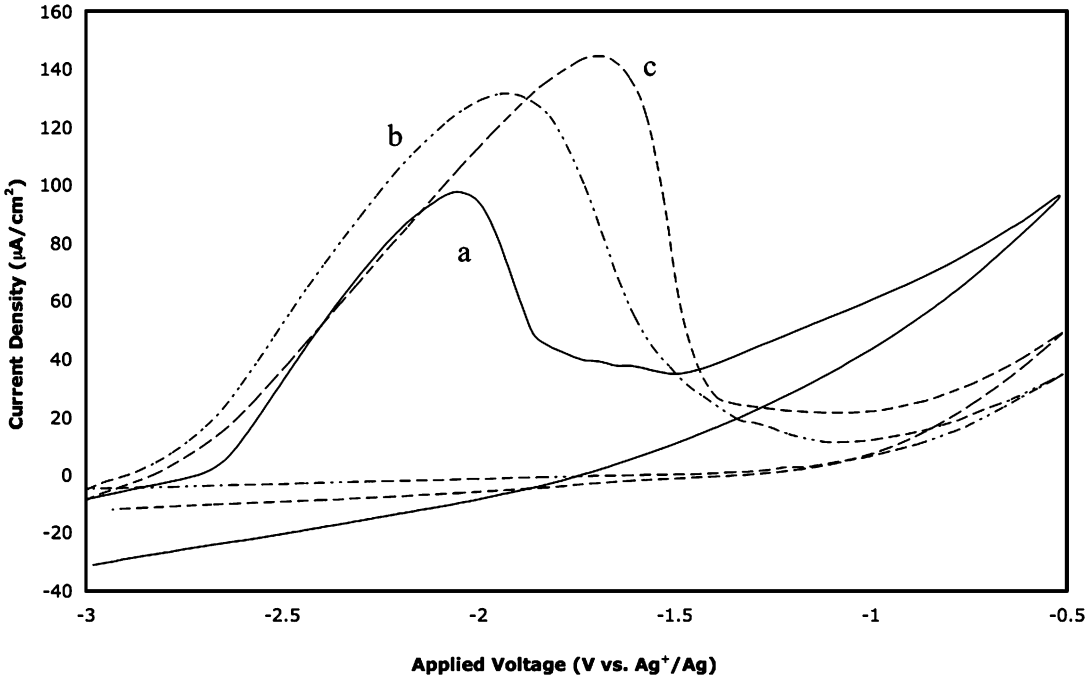

Figure 9. The irreversible oxidation at a Pt working electrode of (a) 1 M CH_3MgCl, (b) 1 M *n*-hexylMgCl, and (c) 1 M phenylMgCl in THF, with 100 mM LiBr.

hydrogen from either the solvent or neighboring surface-bonded alkyl groups which could eventually abstract hydrogen from the solvent. This mechanism explains why the Cl signal is eliminated even for reagents that cannot sterically form Si−C bonds to every atop site on the Si(111) surface.

This reaction mechanism is similar to one proposed recently by Fellah et al. for the reaction of H−Si(111) surfaces with alkyl Grignards.[37] In that mechanism, alkyl halide impurities in the Grignard solution were proposed to be reduced to form alkyl radicals, which attacked the H-terminated surface or halogenated the surface as an intermediate step before reaction with the alkyl Grignard. Although the work was performed on a different surface process than the one considered herein, the mechanistic proposal nevertheless lends support to the notion that electron-transfer processes, followed by single-electron-transfer reactions, provide a viable mechanism for the reactivity of Cl-terminated Si(111) surfaces under the conditions evaluated herein.

C. Electrical and Chemical Passivation of the Si(111) Surfaces by Alkylation. The bulky alkyl groups used herein clearly cannot bond to all Si atop sites on an unreconstructed Si(111) surface. The IR studies described above, as well as electrochemical measurements and related IR studies,[30,38] indicate that a majority of the nonalkylated Si sites form Si−H bonds after the two-step chlorination/alkylation process.

The presence of H-termination of unalkylated Si atop sites offers an explanation for the low initial surface recombination velocities observed for such systems. Unoxidized H-terminated Si(111) surfaces and CH_3-terminated Si(111) surfaces both have low surface recombination velocities. Scanning tunneling spectroscopic studies,[39] as well as UHV-based photoemission studies,[27] have shown that CH_3−Si(111) surfaces have essentially no band bending and no detectable electronic states within the band gap. Additionally, the bond strength of Si−H and Si−C bonds is similar in small molecule models,[40−42] and valence band photoelectron spectroscopic data indicate that the emission energies of CH_3-terminated Si(111) surfaces are similar to those of H-terminated Si(111) surfaces.[27] Thus, even surfaces with mixed Si−C and Si−H functionality would be expected to have relatively few mid-gap states, in accord with the present observations.

The relatively slow oxidation in air of the Si−H sites on Si(111) surfaces alkylated with groups other than CH_3− has been discussed in detail for C_2H_5-terminated surfaces.[28] For the bulky alkyl groups investigated herein, at least partial inhibition of the rate of surface oxidation might be expected due to steric crowding of surficial Si−H bonds by neighboring alkyl groups. This crowding should inhibit the oxidation of the initially unreacted site as well as the oxidation of adjacent surface silicon atoms, because oxygen or water would need to intercalate into the alkyl surface covering or through previously oxidized sites to attack the surface. A modest degree of oxidative protection has been observed by forming self-assembled monolayers with very long chain alkylthiols on Cu.[43] The stark contrast in air oxidation rates of alkylated vs H-terminated Si surfaces indicates that the reaction mechanism involves neighboring Si−H sites or initial oxidation on step edges.[28] Thus, even modest alkyl coverages on the terraces and step edges of functionalized Si(111) surfaces are sufficient to significantly reduce the observed rate of oxidation.

The persistence of a low SRV value even when Si oxide is detected, after extremely long exposures to air, indicates that the oxide that forms on the alkylated surfaces is chemically different from the oxide that (rapidly) forms on the H-terminated surface. A detailed soft XPS study comparing the oxides on H-, CH_3-, and C_2H_5-terminated Si(111) surfaces has revealed that only Si suboxides are formed on alkylated surfaces, whereas SiO_2 forms as a result of the oxidation of H−Si(111) in ambient air.[44] Thus, the different surface chemistry reflects the inertness of the Si−C bonds toward oxidation of both the step edges and terrace sites, and produces a less deleterious, less electrically defective Si oxide on the alkylated surfaces. Hence, the electrical passivation persists even though the chemical oxidation is slowed, but not entirely suppressed, for extended time periods.

V. Conclusions

Alkylation of Si(111) surfaces through a two-step chlorination/alkylation procedure provides both chemical and electrical

passivation of Si surfaces even when bulky alkyl groups are used as alkylating reagents. The intensity of a low binding energy C 1s XPS peak, ascribable to carbon bonded to Si, provided a quantitative estimate of the coverage of alkyls on such surfaces relative to the coverage of methyl groups on CH_3-terminated Si(111) surfaces. Ethyl groups yielded coverages as high as 80% of a monolayer, whereas bulkier groups produced lower coverages, as expected. Even *tert*-butyl groups, which were measured by XPS to bond to only 40% of the surface sites on an unreconstructed Si(111) surface, showed excellent surface passivation, with less than half a monolayer of Si oxide formed on the surface after a three-week exposure to air, and surface recombination velocities <100 cm s^{-1} after that same time period. All of the Cl was removed by reaction even with very bulky alkyl Grignard reagents, and infrared spectroscopy indicated that Si−H bonds were formed on sites that had not been alkylated by the bulky alkyl groups. A viable mechanism for reaction of the Cl-terminated Si(111) surface with alkyl Grignard reagents involves electron transfer between the Grignard reagent and the Cl-terminated Si surface, producing a loss of Cl^- and producing Si radicals that can then react either with alkyls, alkyl Grignards, or abstract H from the solvent to form Si−C bonds or Si−H bonds.

Acknowledgment. We gratefully acknowledge the NSF, Grant CHE-021358 and the Beckman Institute for support of this work.

References and Notes

(1) Linford, M. R.; Fenter, P.; Eisenberger, P. M.; Chidsey, C. E. D. *J. Am. Chem. Soc.* **1995**, *117*, 3145−3155.

(2) Sieval, A. B.; Demirel, A. L.; Nissink, J. W. M.; Linford, M. R.; van der Maas, J. H.; de Jeu, W. H.; Zuilhof, H.; Sudholter, E. J. R. *Langmuir* **1998**, *14*, 1759−1768.

(3) Sieval, A. B.; Linke, R.; Heij, G.; Meijer, G.; Zuilhof, H.; Sudholter, E. J. R. *Langmuir* **2001**, *17*, 7554−7559.

(4) Boukherroub, R.; Morin, S.; Wayner, D. D. M.; Lockwood, D. J. *Phys. Status Solidi A−Appl. Res.* **2000**, *182*, 117−121.

(5) Terry, J.; Linford, M. R.; Wigren, C.; Cao, R. Y.; Pianetta, P.; Chidsey, C. E. D. *Appl. Phys. Lett.* **1997**, *71*, 1056−1058.

(6) Cicero, R. L.; Linford, M. R.; Chidsey, C. E. D. *Langmuir* **2000**, *16*, 5688−5695.

(7) Effenberger, F.; Gotz, G.; Bidlingmaier, B.; Wezstein, M. *Angew. Chem., Int. Ed. Engl.* **1998**, *37*, 2462−2464.

(8) Boukherroub, R.; Morin, S.; Bensebaa, F.; Wayner, D. D. M. *Langmuir* **1999**, *15*, 3831−3835.

(9) Buriak, J. M.; Stewart, M. P.; Geders, T. W.; Allen, M. J.; Choi, H. C.; Smith, J.; Raftery, D.; Canham, L. T. *J. Am. Chem. Soc.* **1999**, *121*, 11491−11502.

(10) Saghatelian, A.; Buriak, J.; Lin, V. S. Y.; Ghadiri, M. R. *Tetrahedron* **2001**, *57*, 5131−5136.

(11) Cicero, R. L.; Chidsey, C. E. D.; Lopinski, G. P.; Wayner, D. D. M.; Wolkow, R. A. *Langmuir* **2002**, *18*, 305−307.

(12) Wacaser, B. A.; Maughan, M. J.; Mowat, I. A.; Niederhauser, T. L.; Linford, M. R.; Davis, R. C. *Appl. Phys. Lett.* **2003**, *82*, 808−810.

(13) Jiang, G. L.; Niederhauser, T. L.; Davis, S. D.; Lua, Y. Y.; Cannon, B. R.; Dorff, M. J.; Howell, L. L.; Magleby, S. P.; Linford, M. R. *Colloids Surf., A* **2003**, *226*, 9−16.

(14) Henry de Villeneuve, C.; Pinson, J.; Ozanam, F.; Chazalviel, J. N.; Allongue, P. *Mater. Res. Soc. Symp. Proc.* **1997**, *451*, 185−195.

(15) Allongue, P.; de Villeneuve, C. H.; Pinson, J.; Ozanam, F.; Chazalviel, J. N.; Wallart, X. *Electrochim.* Acta **1998**, *43*, 2791−2798.

(16) Fidelis, A.; Ozanam, F.; Chazalviel, J. N. *Surf. Sci.* **2000**, *444*, L7−L10.

(17) Webb, L. J.; Lewis, N. S. *J. Phys. Chem. B* **2003**, *107*, 5404−5412.

(18) Bansal, A.; Li, X. L.; Yi, S. I.; Weinberg, W. H.; Lewis, N. S. *J. Phys. Chem. B* **2001**, *105*, 10266−10277.

(19) Royea, W. J.; Juang, A.; Lewis, N. S. *Appl. Phys. Lett.* **2000**, *77*, 1988−1990.

(20) Bansal, A.; Lewis, N. S. *J. Phys. Chem. B* **1998**, *102*, 1067−1070.

(21) Okubo, T.; Tsuchiya, H.; Sadakata, M.; Yasuda, T.; Tanaka, K. *Appl. Surf. Sci.* **2001**, *171*, 252−256.

(22) Bansal, A.; Li, X.; Lauermann, I.; Lewis, N. S.; Yi, S. I.; Weinberg, W. H. *J. Am. Chem. Soc.* **1996**, *118*, 7225−7226.

(23) Dabrowski, J.; Mussig, H. J. *Silicon Surfaces and Formation of Interfaces*; World Scientific Publishing Co. Pte. Ltd.: London, 2000.

(24) Pauling, L. *The Nature of the Chemical Bond*; Cornell University Press: New York, 1960.

(25) Yu, H. B.; Webb, L. J.; Ries, R. S.; Solares, S. D.; Goddard, W. A.; Heath, J. R.; Lewis, N. S. *J. Phys. Chem. B* **2005**, *109*, 671−674.

(26) Seah, M. P. In *Practical Surface Analysis*, 2nd ed.; Briggs, D., Seah, M. P., Eds.; John Wiley & Sons: Chichester, 1990; Vol. 1, pp 201−255.

(27) Hunger, R.; Fritsche, R.; Jaeckel, B.; Jaegermann, W.; Webb, L. J.; Lewis, N. S. *Phys. Rev. B* **2005**, *72*.

(28) Webb, L. J.; Nemanick, E. J.; Biteen, J. S.; Knapp, D. W.; Michalak, D. J.; Traub, M. C.; Chan, A. S. Y.; Brunschwig, B. S.; Lewis, N. S. *J. Phys. Chem. B* **2005**, *109*, 3930−3937.

(29) Miyadera, T.; Koma, A.; Shimada, T. *Surf. Sci.* **2003**, *526*, 177−183.

(30) Webb, L. J.; Rivillon, S.; Michalak, D. J.; Chabal, Y. J.; Lewis, N. S. *J. Phys. Chem. B* **2006**, *110*, 7349−7356.

(31) Atkins, P. W. *Physical Chemistry*, 6th ed.; W. H. Freeman and Company: New York, 1998.

(32) Yuan, S. L.; Cai, Z. T.; Jiang, Y. S. *New J. Chem.* **2003**, *27*, 626−633.

(33) Ashby, E. C.; Bowers, J. R. *J. Am. Chem. Soc.* **1981**, *103*, 2242−2250.

(34) Ashby, E. C.; Bowers, J.; Depriest, R. *Tetrahedron Lett.* **1980**, *21*, 3541−3542.

(35) Blomberg, C.; Salinger, R. M.; Mosher, H. S. *J. Org. Chem.* **1969**, *34*, 2385−&.

(36) Blomberg, C.; Mosher, H. S. *J. Organomet. Chem.* **1968**, *13*, 519−&.

(37) Fellah, S.; Boukherroub, R.; Ozanam, F.; Chazalviel, J. N. *Langmuir* **2004**, *20*, 6359−6364.

(38) Hurley, P. T.; Nemanick, E. J.; Lewis, N. S. To be submitted.

(39) Yu, H. B.; Webb, L. J.; Ries, R. S.; Solares, S. D.; Goddard, W. A.; Heath, J. R.; Lewis, N. S. *Appl. Phys. Lett.*, in press.

(40) Wu, Y. D.; Wong, C. L. *J. Org. Chem.* **1995**, *60*, 821−828.

(41) Kanabus-Kaminska, J. M.; Hawari, J. A.; Griller, D.; Chatgilialoglu, C. *J. Am. Chem. Soc.* **1987**, *109*, 5267−5268.

(42) Walsh, R. *Acc. Chem. Res.* **1981**, *14*, 246−252.

(43) Laibinis, P. E.; Whitesides, G. M. *J. Am. Chem. Soc.* **1992**, *114*, 9022−9028.

(44) Webb, L. J.; Michalak, D. J.: Biteen, J. S.: Brunschwig, B. S.; Chan, A. S. Y.; Knapp, D. W.; Meyer, H. M., III; Nemanick, E. J.; Traub, M. C.; Lewis, N. S. *J. Phys. Chem. B*, submitted for publication.